Exp Brain Res (1996) 108:221–235

RESEARCH ARTICLE

Ronald E. Kettner · Hoi-Chung Leung
Barry W. Peterson

Predictive smooth pursuit of complex two-dimensional trajectories in monkey: component interactions

Received: 23 May 1995 / Accepted: 13 October 1995

Abstract Smooth pursuit eye movements were studied in monkeys tracking target spots that moved two-dimensionally. Complex target trajectories were created by applying either two or three sinusoids to horizontal and vertical axes in various combinations. The chance of observing predictable performance was increased by repeated training on each trajectory. Data analyses were based upon repeated presentations of each trajectory within sessions and on successive days. We wished to determine how accurately monkeys could pursue targets moving along these trajectories and to observe interactions among frequency components. At intermediate frequencies, tracking performance was smooth and consistent during repeated presentations with saccadic corrections that were well integrated with smooth pursuit. The mean gain for eight different sum-of-sines trajectories was 0.83 and the mean magnitude (absolute value) of the phase error was 6°. In light of the long delays that have been associated with the processing of visual information, these values indicate that the monkeys were pursuing predictively. Five factors influenced predictive pursuit performance: (1) there was a decline in performance with increasing frequency; (2) horizontal pursuit was better than vertical pursuit; (3) high-frequency components were tracked with higher gains and phase lags, while lower-frequency components were tracked with lower gains and phase leads; (4) the gain of sinusoidal pursuit was always reduced when a second sinusoid was applied to the same axis or, to a lessor extent, when a second sinusoid of higher frequency was applied to the orthogonal axis; (5) the phase of sinusoidal pursuit shifted from a phase lag to a phase lead when combined with a second sinusoid of higher frequency, but was not affected by the addition of a lower-frequency sinusoid. Findings 1 and 2 confirm, in monkeys, results reported for humans, and 3 extends to monkeys and to two-dimensional pursuit results based upon human subjects. All of these findings demonstrate that complex predictive tracking is controlled by a nonlinear and nonhomogeneous system that uses predictive strategies in concert with feedback control to generate good pursuit.

Key words Smooth-pursuit eye movements · Prediction · Nonlinear interactions · Monkey

R. E. Kettner (✉) · H.-C. Leung · B. W. Peterson
Institute for Neuroscience and Department of Physiology, Northwestern University Medical School, Chicago, IL 60611, USA;
Fax: +1-312-503-5101; e-mail: r-kettner@nwu.edu

Introduction

Smooth pursuit eye movements allow tracking of a moving visual target so that the target image remains near the fovea of the eye. Past studies of pursuit behavior indicate that the system is highly accurate, showing little or no time lag between target and eye movement at low velocities, or when the target travels along a highly predictable trajectory. For example, when a target moves back and forth at a constant frequency, pursuit eye movements soon synchronize with the stimulus so that transitions are made with zero lag (Dallos and Jones 1963; Lisberger et al. 1981; Bahill and McDonald 1983). Pursuit at small lags is called predictive pursuit because a number of studies (Robinson 1965; Fuchs 1967; Becker and Fuchs 1984; Van den Berg 1988; Leung et al. 1994; Leung and Kettner 1995) have indicated that visual information about target location is delayed by 100–200 ms before it is used to make changes or corrections in pursuit. To compensate for this relatively long delay, the brain systems that generate pursuit appear to utilize consistencies in the target trajectory that allow the prediction of target position and velocity 100–200 ms in the future.

Most of the paradigms that have been used to study predictive pursuit are based upon targets undergoing relatively simple target motions. These include one-dimensional constant velocity ramps (Rashbass 1961), sinusoidal (Dallos and Jones 1963; Lisberger et al. 1981; Bahill and McDonald 1983) or square-wave (Kowler and Steinman 1979; Pola and Wyatt 1980) trajectories, and two-dimensional tracking along a constant-velocity circular trajectory (Collewijn and Tamminga 1984; Leung et al.

1994; Leung and Kettner 1995). Several investigators have also argued that pseudorandom trajectories restricted to the horizontal axis composed of 16 sinusoids (Yasui and Young 1984) or created using Gaussian random noise (Dallos and Jones 1963) can be tracked with varying degrees of prediction. Barnes et al. (1987) emphasized that the high-frequency component of sum-of-sines trajectories restricted to the horizontal axis are tracked predictively in terms of gain. The present study set out to characterize predictive pursuit during complex two-dimensional trajectories created by summing either two or three sinusoids along horizontal and vertical axes. We attempted to increase the chances for observing predictive control by training each monkey for a period of several weeks before data collection commenced, and found that all the trajectories were tracked with small lags indicative of predictive pursuit.

Trajectories created from simple combinations of sinusoids facilitated the analysis of complex pursuit. Short waveform periods were obtained using two- or three-component frequencies that were related by small-integer ratios. This allowed the repetition of each complex waveform so that pursuit strategies that were invariant across repetitions could be studied. In particular, it was possible to overlay individual repetitions of the same trajectory and to observe consistencies in pursuit errors and saccadic corrections. Because components had different frequencies, high- versus low-frequency tracking could be compared. Barnes and colleagues (Barnes et al. 1987; Barnes and Ruddock 1989) have shown for human subjects that the high-frequency component is tracked with the highest gain for sum-of-sines waveforms restricted to the horizontal axis; and others (Yasui and Young 1984; Collewijn and Tamminga 1984; Barnes et al. 1987; Barnes and Ruddock 1989) have shown that low-frequency components are tracked with a slight phase lead, while high-frequency components are tracked with phase lags. The present experiments were designed to extend these results in monkeys to complex, two-dimensional trajectories that could be tracked predictively.

Component analyses of two-dimensional tracking also allowed the study of interactions between the processing of horizontal and vertical inputs. It is logically possible that horizontal and vertical pursuit could have been controlled independently. In support of this idea is physiological evidence for a division of smooth eye movement effector systems into horizontal and vertical divisions (Fuchs and Kimm 1975; Lisberger and Fuchs 1978a, b; Miles et al. 1980; Balaban et al. 1981; Chubb and Fuchs 1982; Balaban and Watanabe 1984; Chubb et al. 1984; Tomlinson and Robinson 1984; Belknap and Noda 1987; Stone and Lisberger 1990a, b; Sato and Kawasaki 1991; McFarland and Fuchs 1992; Scudder and Fuchs 1992). This hypothesis was tested by comparing the pursuit of a single sine wave presented on one axis with the same stimulus presented in combination with another sinusoid on either the same or the orthogonal axis. In another set of experiments, we compared the pursuit of a sum-of-two-sines waveform presented along one axis and then in combination with a third sine wave presented along either the same or the orthogonal axis.

Materials and methods

Two adult male rhesus monkeys (*Macaca mulatta*; 4–6 kg) were used in the experiments. They were cared for and housed by the Northwestern University Center for Experimental Animal Resources according to *Principles of laboratory animal care* (NIH publication No. 86–23, revised 1985). A variety of supplemental foods and toys were provided to enrich their environment and improve their well being. They appeared to enjoy the regimen of coming out of their cage each day, riding to the experimental room, and performing in the experiments. Care was taken to develop a rapport with the animals and training occurred at a slow enough pace so that the animals always performed with a minimum of errors and were not under undue stress.

Surgery

Before surgery, each monkey was immobilized with ketamine hydrochloride (10 mg/kg i.m.) during shaving, cleaning, and application of disinfectant surgical scrub. Aseptic surgery was done under deep anesthesia induced by sodium thiamylal (20 mg/kg i.v.) and maintained with halothane (1%) administered via an endotracheal tube. Under aseptic conditions an oval of skin was resected and the underlying cranium scraped clean of periosteal tissue. A stainless steel assembly used to fix the head during the experiment was anchored with dental acrylic secured by stainless steel screws partially threaded into the bone. An eye coil was implanted under the conjunctiva of one eye (Robinson 1963; Judge et al. 1980), with its connecting wires led under the skin to an electrical plug positioned near the fixation assembly and secured with dental acrylic. The exposed bone, fixation assembly, and eye-coil plug were covered with a smoothed layer of acrylic. For 1 week after surgery the monkey was given daily doses of cephalothin (15 mg/kg i.m.) and an antibiotic salve applied topically to prevent infection. Analgesia was maintained with topical applications of lidocaine each day until the incision had healed and during the first 4 days following surgery by injections of buprenorphine hydrochloride (0.01 mg/kg i. m.).

Apparatus

The pursuit stimulus was a laser spot back-projected onto a tangent screen that measured 60° by 60° located 40 cm from the monkey's eyes. The spot on the screen was 5 mm in diameter with a luminance of 92 cd/m^2 against a background of less than 2 cd/m^2. Its location was controlled by a pair of servo-controlled mirror galvanometers (General Scanning, Watertown, Mass.). Mirror position signals were generated by the 12-bit digital-to-analog converter of the computer and then filtered with an 8-pole, low-pass Bessel filter with a cutoff frequency of 100 Hz. Our computer program used a 1000-point waveform per cycle and then put out multiple cycles at different rates to generate the experimental stimulus. Output rates ranged from 3000 samples/s at 3.0 Hz to 100 samples/s at 0.1 Hz. During the experiment the monkey was seated in a primate chair with its head fixed at the center of 90 cm magnetic coils. Eye position was monitored by a magnetic search coil system (CNC Engineering). Horizontal eye position was monitored using phase differences relative to a reference coil mounted 3 cm from the eye coil for a rotating electromagnetic field vector (Collewijn et al. 1975). Vertical eye position was based upon amplitude changes in induced eye-coil current (Robinson 1963); these were not corrected for cosine error owing to the small visual angles used. Eye position measurements were accurate to 15 min arc for the range of eye movements studied.

Horizontal and vertical eye position as well as horizontal and vertical mirror position signals were filtered with 8-pole, low-pass

Bessel filters with cutoff frequencies at 500 Hz. These signals were then digitized at 1000 Hz using the 12-bit analog-to-digital converter of the computer. Spot position signals were calibrated each day both statically (horizontal, vertical, and diagonal locations of 0°, ±5°, and ±10°) and dynamically (5° and 10° circles) relative to traces on a moveable calibration screen that was in contact with the viewing screen during calibrations and was then moved away during the experiment. Eye position calibrations were conducted at the beginning of each day based upon fixation and pursuit of the above calibration stimuli. Offset and gain values were first set so that center position was zero and ±10° was ±1000 analog-to-digital units. Calibration runs based upon these settings were then stored by computer. Although calibrations were tested each day, they were very stable across time in terms of gain, with only slight changes in offset each day.

Calibration, training, and experimental runs utilized custom software that allowed real-time monitoring of pursuit performance and automated reward delivery. The computer displayed eye and target position as well as ±2° rectangular error windows for each trace. Reward delivery by computer occurred at set points on the stimulus waveform when the monkey had tracked the target within the window limits for more than 500 ms. As indicated in the results, well-trained animals had much smaller errors, and at all but the highest frequencies stayed within the error window during an entire run of 5–20 waveform cycles.

Training

The monkeys underwent extensive training before data collection began. Several weeks were required to accustom each monkey to the experimental apparatus and to train him to associate correct tracking performance with reward delivery. During the initial phase of the training, larger error windows were used and shorter fixation times were required for reward delivery. Additional weeks were required to obtain extended performance under multiple tracking conditions at a variety of waveform frequencies. The monkeys were trained until gain and phase values were stable for several days before we collected data for analysis from five daily sessions. Although we did not systematically study the acquisition of smooth pursuit behavior in the paradigms described below, there were clear improvements in performance over the course of training. These enhancements were not due to a lack of familiarity with the experimental surroundings or a misunderstanding of the pursuit task. When the monkeys were switched from sum-of-two-sines tracking to sum-of-three-sines stimuli after obtaining considerable experience in the task, there were clear improvements over days after repeated presentations of the new stimulus. In sum, there were clear practice effects that we attempted to eliminate by studying pursuit performance after it had reached asymptotic levels.

Waveform terminology and description

In descriptions of complex sum-of-sines waveforms, the following terminology is used. The frequency of the complex waveform is called the "waveform frequency" to contrast it from the frequencies of its components, called "component frequencies". The waveform frequency is the repeat rate of the trajectory created by the complex waveform. For example, H2H3 indicates a sum-of-two-sines waveform created with horizontal (H) components at 2 and 3 times the waveform frequency. H4H6V7 refers to a sum-of-three-sines trajectory created by adding two horizontal components and one vertical (V) component with frequencies 4, 6, and 7 times the waveform frequency. Individual components within a sum-of-sines waveform will be indicated with parentheses. For instance, the V6 component of the waveform V4V6H7 will be referred to as V4(V6)H7.

To facilitate comparisons among the components of sum-of-sines waveforms, components were equated with respect to peak velocity. This was accomplished by making the amplitude (A) of the slowest frequency component equal to 5° and the amplitudes of higher-frequency components smaller so that the peak velocity (P) at a particular frequency (f) was a constant given the relationship $P=2\pi Af$. Thus, the V2H3 waveform had components with amplitudes of 5° and 3.33° and frequencies of 2.0 Hz and 3.0 Hz, respectively, and shared a common peak velocity of 31.4°/s at the waveform frequency of 1.0 Hz.

Data analysis

Two-dimensional eye position traces, as well as the horizontal and vertical components of these eye position traces were displayed as overlaid waveforms (see Fig. 1). The same display included eye velocity traces computed from position data using digital smoothing (50-point Gaussian) followed by symmetric differentiation. Pursuit performance of a sum-of-sines trajectory was quantified in terms of its components. Thus, the V4V6H7 wave had three gain-phase pairs associated with each of its three components: (V4)V6H7, V4(V6)H7, and V4V6(H7). Gain was the ratio of eye and target velocity, and perfect tracking corresponded to a gain of 1.0. Phase was the time difference between eye and target velocity measured as an angle. Positive phase values corresponded to the eye leading the target, while negative phases indicated the eye lagging the target.

Measurement of pursuit gain and phase were obtained using custom software that allowed the display and user-controlled deletion of saccades, as well as sinusoid regression fits of saccade-edited eye-velocity and target-velocity traces at user-specified frequencies. Multiple-component waveforms were analyzed by fitting multiple sinusoids to saccade-edited eye velocity and target velocity data. For example, H2H3 traces presented at 0.2 Hz were fit first with a sinusoid at 0.4 Hz and then with a sinusoid at 0.6 Hz. This resulted in a gain and phase for the 0.4-Hz component and a gain and phase for the 0.6-Hz component. This procedure is equivalent to estimating the discrete Fourier components of the sum-of-two-sines waveform at 0.4 Hz and 0.6 Hz. Because our eye records had missing data points where saccades had been deleted, we did not use the fast Fourier transform (FFT) that requires 2^n equally spaced data points. Rather, our technique is related to algorithms for estimating Fourier components from data that is not sampled at equal intervals because of missing data (Press et al. 1992). These algorithms estimate the Fourier component at a particular frequency by performing a sine fit at the frequency of the Fourier component to be estimated. Following the example of others (Collewijn and Tamminga 1984;Yasui and Young 1984; Barnes et al. 1987), we did not compute Fourier components at frequencies other than those used to construct the trajectories. When we initially performed traditional FFTs on the data, there were no discernible energy peaks at higher frequencies, in agreement with Yasui and Young (1984).

Statistically significant differences among sets of gain and phase curves were determined using two-way (frequency×trajectory) analyses of variance (ANOVA) with replication (Winer et al. 1991). To standardize analyses, the same number of replications (n=10: two monkeys×five runs) were used for each analysis. Post-hoc comparisons among trajectory means were based upon the Tukey honestly significant difference (HSD) technique (Winer et al. 1991). The HSD defines a significant difference between means that have been shown to have significant variation using ANOVA. These differences take into account the increased errors that arise from repeated tests. A significance level of $P<0.05$ was used to define significant differences for both ANOVA and HSD tests.

Sum-of-sines trajectories were analyzed at three standard waveform frequencies: 0.3, 0.4, and 0.5 Hz for sum-of-two-sines trajectories, and 0.05, 0.10, and 0.15 Hz for sum-of-three-sines trajectories. These values were selected because they were the three highest frequencies for which consistent behavior was observed across all waveforms studied over a period of several days in both animals. This allowed statistical analyses based upon analysis of variance with replication. Lower frequencies were not studied in detail. In the limit as the presentation frequency declines to very low values, one

expects gain and phase values to approach optimal values. This result was supported by preliminary runs at lower frequencies on the first monkey that showed gain and phase values all within a range from 0.9 to 1.0 or near-zero lag with component differences that were small compared with measurement variability. In addition, the monkeys did not work at very low frequencies because they received less reward per second than at higher frequencies, and this increase in reward would have made it difficult to collect a full set of data in the restricted time period of a daily session. Data collection at higher frequencies was limited by a refusal to perform without reward when fixation was not maintained. This refusal was probably associated with poor tracking and not reward delivery, because the monkeys refused to track during runs with a reduced fixation interval and even when we gave free rewards. Thus, we studied pursuit at intermediate frequencies that the monkey performed at consistently from session to session. To allow comparisons between horizontal and vertical pursuit at the same frequencies, we selected frequencies that were one or two steps below the maximum frequencies that were consistently attempted by the animals during horizontal pursuit and one step below the maximum frequencies attempted for vertical pursuit.

Results

Good pursuit performance in terms of both gain and phase was observed for both sum-of-two-sines and sum-of-three-sines trajectories at intermediate tracking frequencies. In addition, consistent pursuit strategies and interactions among pursuit components were observed that may illuminate some of the mechanisms that control pursuit. Pursuit at very low frequencies was not studied, because initial runs and work by others indicated that gain and phase values for all components were clustered near optimal values. Any component differences at low frequencies would have been smaller than the experimental variations observed from session to session. Instead we concentrated our data collection at four or five intermediate frequencies where both monkeys showed

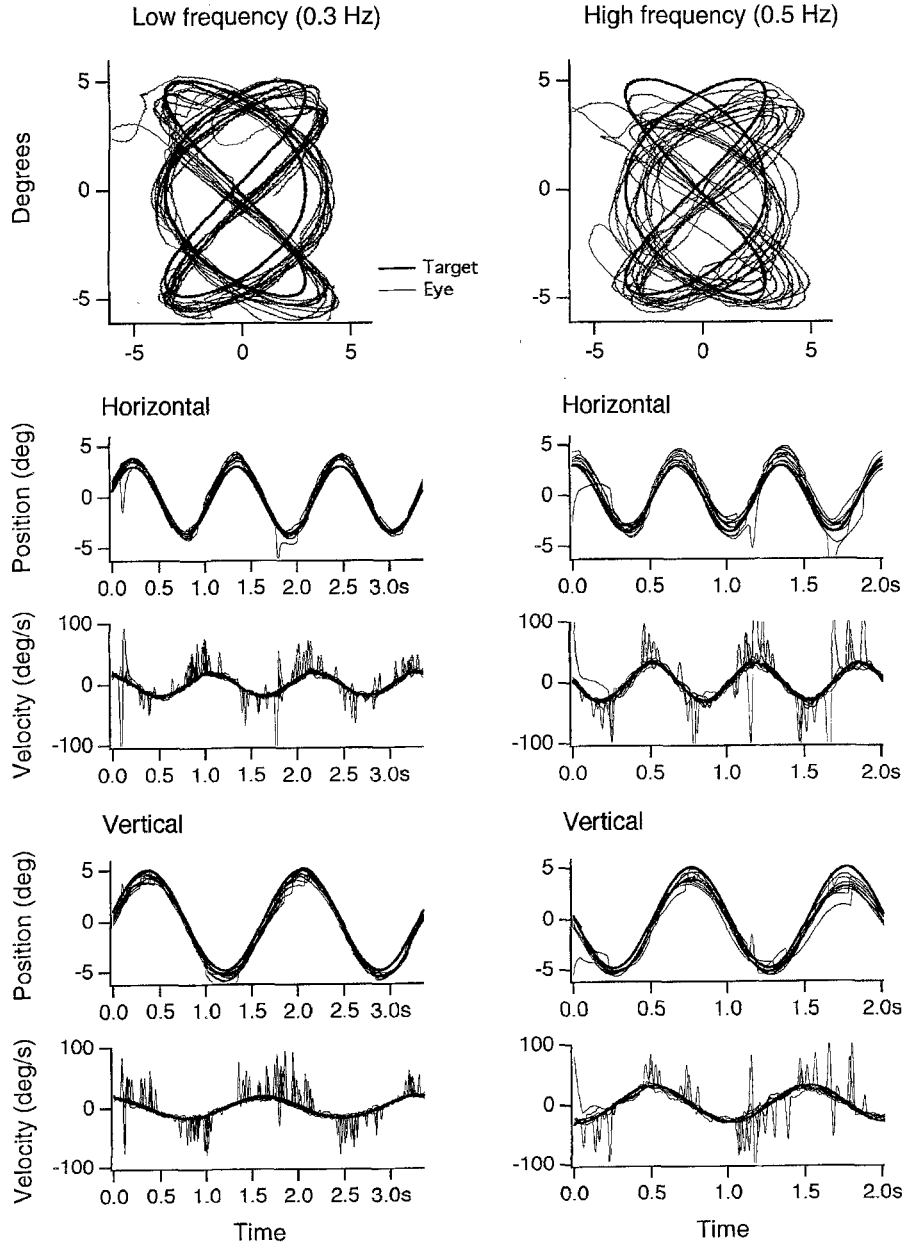

Fig. 1 Pursuit during tracking of the sum-of-two-sines trajectory H3V2 was good at waveform frequencies of 0.3 and 0.5 Hz. The *top panels* show the two-dimensional (2D) trajectories of the target with ten eye traces. *Below* are corresponding component plots of: horizontal position, horizontal velocity, vertical position, and vertical velocity. Target trajectories are indicated by *heavy lines* and eye traces are shown with *thin lines*. Note the smoothness and consistency of pursuit. Deviations from the correct path were consistent across repetitions in 2D traces. Saccades were most common at points of high velocity and were made in the direction of ongoing pursuit, as indicated by *upward* velocity spikes at velocity peaks and *downward* velocity spikes at velocity minima

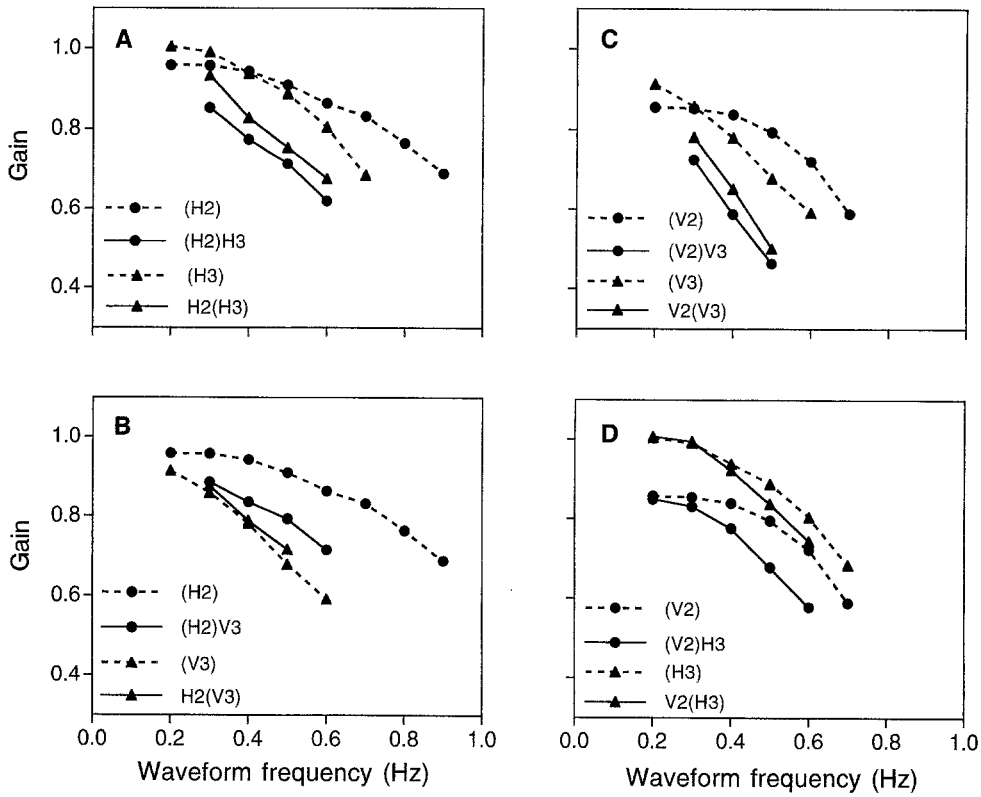

Fig. 2A–D Gain comparisons between the high- and low-frequency components used to construct sum-of-two-sines waveforms, as well as comparisons with single sinusoids at component frequencies. Data related to each waveform frequency at a specific waveform frequency are lined up vertically. For example, in **A** the four points plotted at 0.4 Hz correspond to the mean gain for: low-frequency single sinusoids at 0.8 Hz [*dashed line with circles*; (H2)], low-frequency components at 0.8 Hz for waveforms at 0.4 Hz [*solid line with circles*; (H2)H3], high-frequency single sinusoids at 1.2 Hz [*dashed line with triangles*; (H3)], and high-frequency components at 1.2 Hz for waveforms at 0.4 Hz [*solid line with triangles*; H2(H3)]. The components used to compute gains are in *parentheses*. The waveforms analyzed in each panel are: **A** H2H3, **B** H2V3, **C** V2V3, **D** V2H3

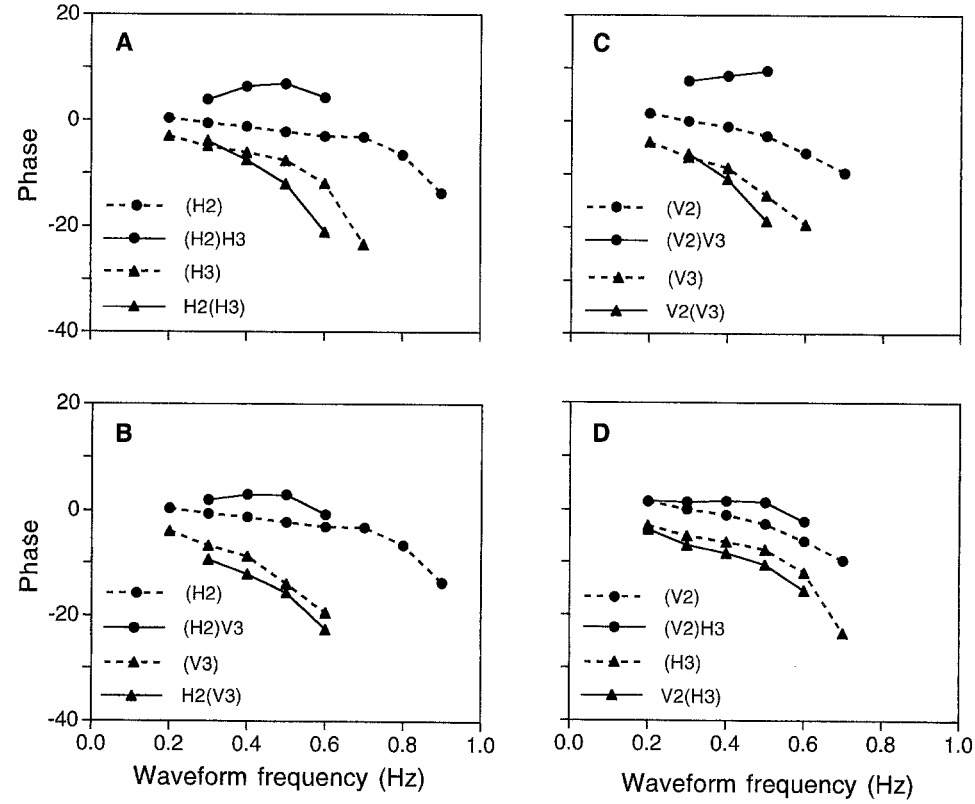

Fig. 3A–D Phase comparisons between the high- and low-frequency components used to construct sum-of-two-sines waveforms, as well as comparisons with single-sinusoids at component frequencies. Symbols are the same as in Fig. 2. Data related to each waveform frequency at a specific waveform frequency are lined up vertically. For example, in **A** the four points plotted at 0.4 Hz correspond to the mean phase for: low-frequency single sinusoids at 0.8 Hz [*dashed line with circles*; (H2)], low-frequency components at 0.8 Hz for waveforms at 0.4 Hz [*solid line with circles*; (H2)H3], high-frequency single sinusoids at 1.2 Hz [*dashed line with triangles*; (H3)], and high-frequency components at 1.2 Hz for waveforms at 0.4 Hz [*solid line with triangles*; H2(H3)]. The components used to compute phases are in *parentheses*. The waveforms analyzed in each panel are: **A** H2H3, **B** H2V3, **C** V2V3, **D** V2H3

Table 1 Two-way ANOVA results for the sum-of-two-sines experiments. Values at the left side of the table are means (based on three frequencies×two monkeys×five repetitions) for performance along specific trajectories across a standard set of waveform frequencies at 0.3, 0.4, and 0.5 Hz. Each mean corresponds to a specific curve for component gain (Fig. 2), component phase (Fig. 3), interaction gain (Fig. 4), and interaction phase (Fig. 5). Each line of the table corresponds to one of the 16 ANOVA tests that were performed. Statistically significant differences among means on a line are indicated by a probability (*P*) value of less than 0.05 for the trajectory factor based upon an *F*-test. Similarly, statistically significant differences among frequency means (not shown) are indicated by a *P* value of less than 0.05 for the frequency factor. When compared trajectories were statistically different, honestly significantly different (HSD) values based upon the mean square (*MS*) error of the trajectory factor were used to determine statistically significant differences among individual means. That is, a difference between two means on a line was statistically significant if it was greater than the HSD (*NS* trajectory effect was not significant and an HSD could not be defined)

	Trajectory	Components						Trajectory		Frequency	
		Low sine	Low comp	High sine	High comp	HSD	MS error	$F_{3,108}$	*P*	$F_{3,108}$	*P*
Gains	H2H3	0.936	0.789	0.930	0.846	0.063	0.008	17.9	0.00	16.7	0.00
	H2V3	0.936	0.832	0.760	0.776	0.076	0.012	15.3	0.00	13.3	0.00
	V2V3	0.809	0.586	0.760	0.638	0.115	0.028	11.4	0.00	13.4	0.00
	V2H3	0.809	0.733	0.930	0.909	0.072	0.011	22.6	0.00	15.8	0.00
Phases	H2H3	−1.4	6.1	−6.6	−7.2	3.2	21.3	53.6	0.00	2.4	0.10
	H2V3	−1.4	2.0	−10.4	−13.1	3.7	29.1	53.1	0.00	5.9	0.00
	V2V3	−1.6	8.9	−10.4	−12.2	4.5	43.1	65.1	0.00	7.5	0.00
	V2H3	−1.6	1.3	−6.6	−9.4	3.3	24.0	28.8	0.00	3.8	0.00

	Trajectory	Interactions								
		Alone	+Same	+Orthogonal						
Gains	H2	0.936	0.789	0.832	0.056	0.008	21.1	0.00	8.7	0.00
	H3	0.930	0.846	0.909	0.056	0.008	7.0	0.00	21.5	0.00
	V2	0.809	0.586	0.733	0.094	0.023	16.6	0.00	8.9	0.00
	V3	0.760	0.638	0.776	0.100	0.026	6.6	0.00	13.0	0.00
Phases	H2	−1.4	6.1	2.0	1.5	6.0	71.0	0.00	1.2	0.30
	H3	−6.6	−7.2	−9.4	NS	42.0	1.5	0.23	4.6	0.00
	V2	−1.6	8.9	1.3	2.2	12.2	72.4	0.00	0.6	0.50
	V3	−10.4	−12.2	−13.1	NS	61.8	1.0	0.39	10.5	0.00

consistent performance from day to day. The maximum frequency studied quantitatively was one or two frequency steps below the very highest frequencies initially attempted by the animals (see Materials and methods).

Sum-of-two-sines pursuit

Examples

In the first set of experiments, four sum-of-two-sines trajectories were studied: H2H3, V2V3, H2V3, V2H3. Each was created by combining sinusoids with a frequency ratio of 2 to 3 on the horizontal and/or vertical axis. To reduce velocity effects, the two components were equated for velocity. Examples of tracking performance for the H3V2 trajectory at 0.3°Hz and 0.5 Hz are shown in Fig. 1, where target traces are represented by thick lines and eye traces are shown as thin lines. Notice the consistent and smooth pattern of pursuit across repeated trajectories. Overshoots at turn-around points were similar across cycles, and, when corrective saccades did occur, they were well integrated into the flow of ongoing pursuit. Although saccades were clearly apparent as spikes in velocity traces, they were not as readily apparent in the one- and two-dimensional position traces. This is due to the increased frequency of saccadic corrections in the direction of ongoing movement near points of high velocity, with only occasional corrections perpendicular to the direction of movement. These saccades are most apparent in velocity traces, where they appear as upward velocity spikes at velocity peaks and as downward velocity spikes at velocity minima. In both cases, corrective saccades were used to increase velocity in the direction of ongoing pursuit. Similar results were obtained for the other three trajectories.

Overall performance

All trajectories were tracked accurately at low frequencies, followed by a decline in performance with increasing frequency. This is illustrated by the gain-frequency curves in Fig. 2 and by the phase-frequency curves in Fig. 3. Results are plotted in terms of waveform frequency so that data from the components of individual waveforms, as well as comparison sinusoids presented alone, line up vertically. Mean values of gain and phase across trajectories are based upon the means for individual trajectories in Table 1 at three frequencies: 0.3, 0.4, and 0.5 Hz. Statistically significant differences between components are based upon ANOVA results from Table 1.

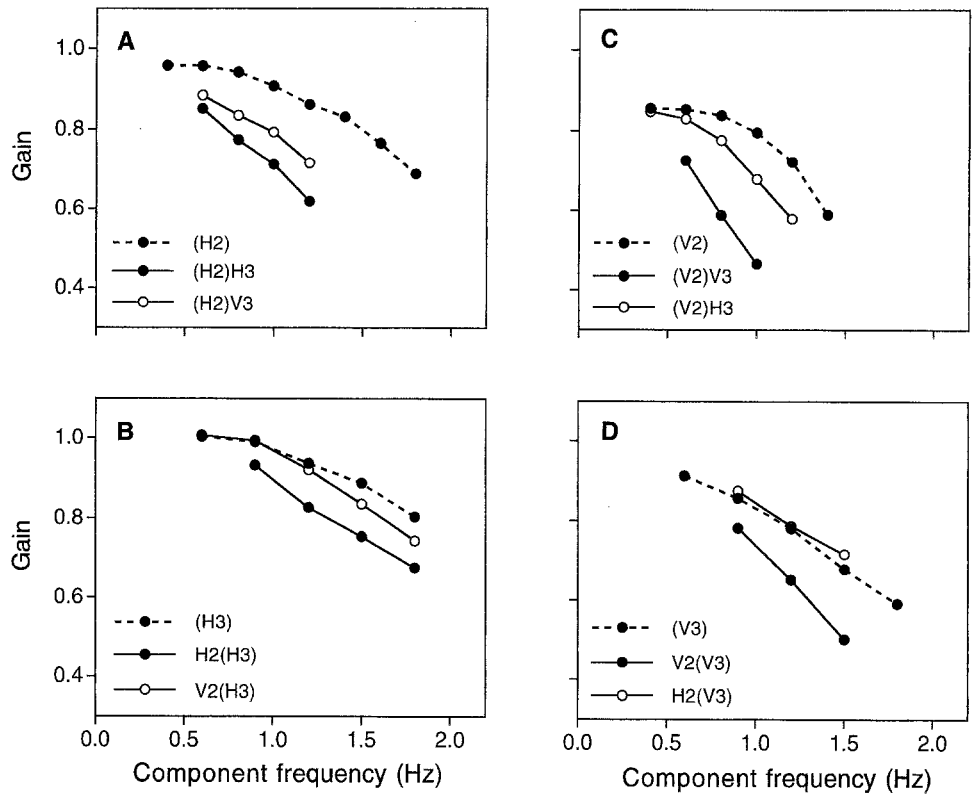

Fig. 4A–D Gain effects on a single sinusoid when a second sinusoid is added to the orthogonal or the same axis. In each panel the *three lines* indicate the gain of the sinusoid when presented: alone (*dashed line with filled circles*), with a second sinusoid on the same axis (*solid line with filled circles*), or with a second sinusoid on the orthogonal axis (*solid line with empty circles*). Components used to compute gains are in *parentheses*. The waveforms analyzed in each panel are: **A** H2, **B** H3, **C** V2, **D** V3

The mean gain across the four trajectories was 0.74 for low-frequency components and 0.79 for high-frequency components. Both values indicate good tracking relative to a perfect gain value of 1.00. On average, the high-frequency components showed a phase lag of 10° and the low-frequency components showed a phase lead of 5°. These phase values were close to values for perfect tracking of 0°. At least four variables controlled pursuit performance: frequency, horizontal versus vertical axis, high- versus low-frequency component, and interactions among these variables.

Frequency effects

As observed in other experiments, there were declines in gain and increases in the magnitude (absolute value) of phase with increasing frequency. These effects were always statistically significant for gain (Table 1) and were also significant for phase, except for the H2H3 waveform, where increases in phase lead for (H2)H3 canceled increases in lag for the H2(H3), H2, and H3 curves.

Horizontal versus vertical axis effects

A second variable controlling pursuit performance was the presentation axis: pursuit was consistently more difficult along the vertical axis. The worst values of gain and phase were obtained for the purely vertical trajectory, V2V3, with mean gains of 0.59 and 0.64 for low- and high-frequency components from Table 1. These values were well below corresponding H2H3 values of 0.79 and 0.85. Similarly, V2V3 phase shifts of 9° and –12° were larger in magnitude than H2H3 values of 6° and –7°. All other factors being equal, horizontal and vertical components follow this relationship:

$$\text{Gain(Horizontal)} > \text{Gain(Vertical)}$$
$$|\text{Phase(Vertical)}| > |\text{Phase(Horizontal)}|$$

Note that the second relationship only works for the magnitude of the phase. Factors determining the sign of the phase are discussed below. We stress that these and other inequalities below serve only to summarize the empirical data succinctly and are not designed to suggest the quantification associated with a detailed mathematical model of pursuit.

High- versus low-frequency component effects

A third factor affecting pursuit was the relative frequency of a component: the high-frequency component was usually tracked with a higher gain than the low-frequency component. The only exception to this rule was for the H2V3 trajectory, which showed a somewhat higher gain for the low-frequency horizontal component at 0.83 compared with 0.78 for the high-frequency vertical component. Here higher gains for horizontal tracking offset the tendency for the low-frequency component to be tracked with lower gain.

A more consistent result was obtained for differences between the gains of high- and low-frequency compo-

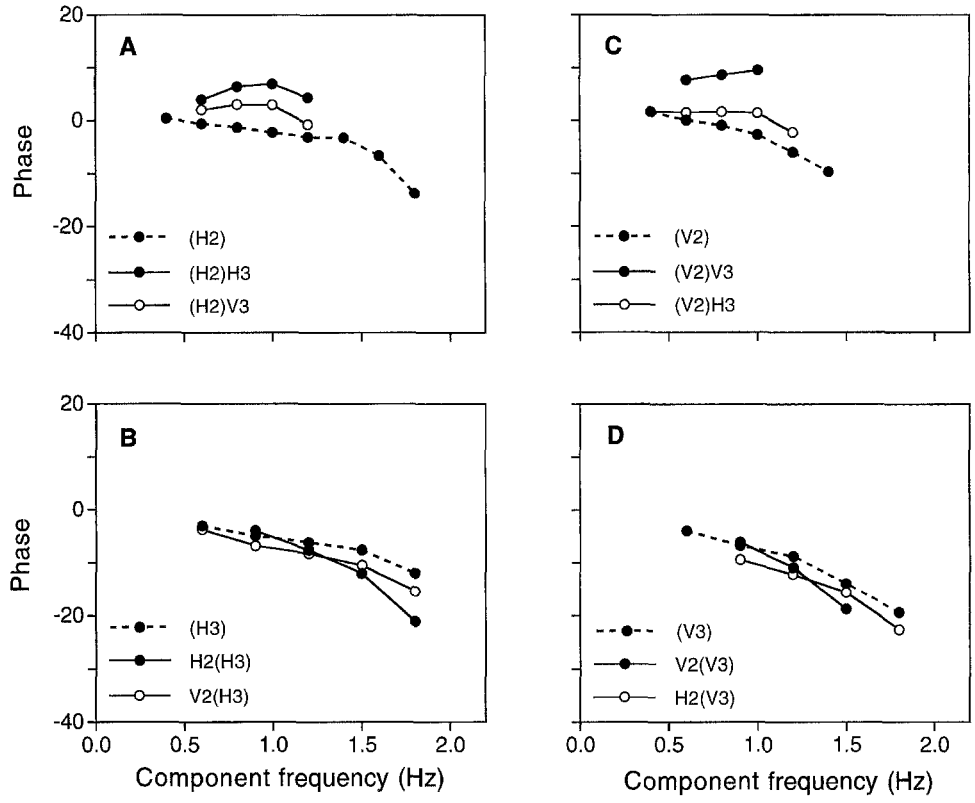

Fig. 5A–D Phase effects on a single sinusoid when a second sinusoid is added to the orthogonal or the same axis. Symbols are the same as for Fig. 4. In each panel the *three lines* indicate the phase of the sinusoid when presented: alone (*dashed line with filled circles*), with a second sinusoid on the same axis (*solid line with filled circles*), or with a second sinusoid on the orthogonal axis (*solid line with empty circles*). Components used to compute phases are in *parentheses*. The waveforms analyzed in each panel are: **A** H2, **B** H3, **C** V2, **D** V3

nents compared with single-sinusoid gains at the same frequencies and amplitudes. When single-sinusoid gain values were subtracted from corresponding components of sum-of-sines stimuli, the following relationship summarizes the results:

$$|\Delta\text{Gain(Low)}| > |\Delta\text{Gain(High)}|$$

Here Δ indicates the change in component gain relative to single-sinusoid values (component gain–single-sinusoid gain). The equation specifies that the largest changes in gain (in this case reductions) were observed for low-frequency components.

There was also a clear lag-lead relationship for the phases of component pairs. The high-frequency component was tracked with a phase lag, while the low-frequency component was associated with a phase lead. Phase leads were never observed when sinusoids were tracked alone. That is, the addition of a high-frequency component changed the phase of low-frequency tracking from a phase lag to a phase lead. Furthermore, the phase lag of the high-frequency component was often increased to an even greater phase lag with the addition of a second sinusoid of lower frequency. The following inequalities capture these relationships:

$$\text{Phase(Low)} > 0 > \text{Phase(High)}$$
$$\Delta\text{Phase(Low)} > 0 > \Delta\text{Phase(High)}$$

Interaction effects

Interactions among components were studied by comparing the effects of adding a same-axis versus an orthogonal-axis component to a single sinusoid. Figure 4 shows gain-frequency plots of sinusoids presented alone (broken lines) and in combination with a second sinusoid applied to the same axis (solid lines with closed circles) or the orthogonal axis (solid lines with open circles). A consistent set of patterns was observed for the low-frequency components, H2 and V2. The gain of a low-frequency sinusoid presented alone, was always greater than the gain of the same sinusoid paired with a higher-frequency component on the orthogonal axis, which, in turn, was greater than when they were paired on the same axis. The following inequality summarizes these relationships:

$$\text{Gain(Low alone)} > \text{Gain(Low+Orthogonal)} > \text{Gain(Low+Same)}$$

A related but somewhat different pattern was observed for the high-frequency components H3 and V3. Their gains were significantly reduced when paired with same-axis sinusoids, but were not significantly reduced when paired with orthogonal-axis sinusoids (Table 1 indicates that these differences were always less than the HSD). These relationships are specified by:

$$\text{Gain(High alone)} \approx \text{Gain(High+Orthogonal)} > \text{Gain(High+Same)}$$

Significant interaction effects were observed for the phase of low-frequency components, but were not observed for high-frequency components. Results are shown in Fig. 5 for the four different trajectories. When presented alone, sinusoids were always tracked with a phase lag. This lag was changed to a lead when a higher-frequency

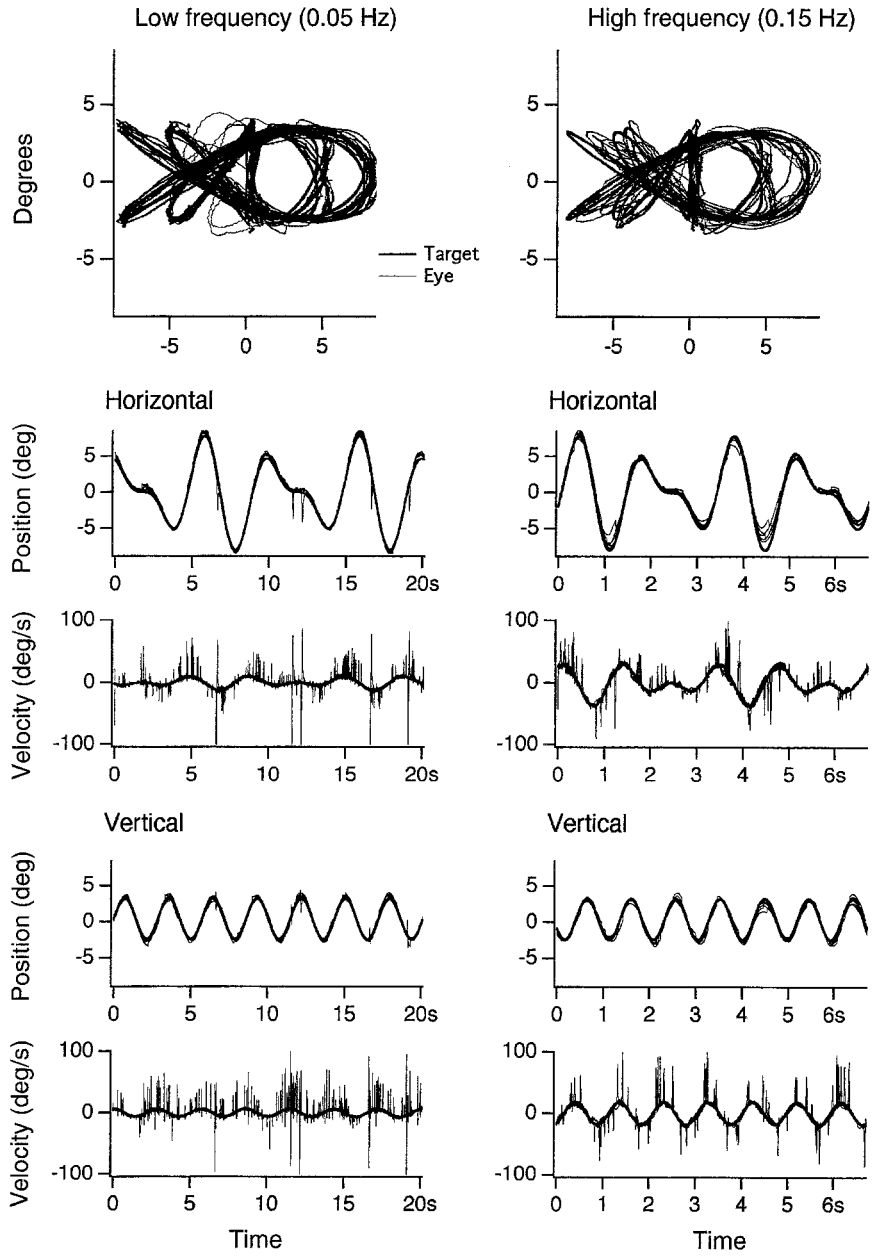

Fig. 6 Pursuit during tracking of the sum-of-three-sines trajectory H4H6V7 at waveform frequencies of 0.05 Hz and 0.15 Hz. The *top panels* show the two-dimensional trajectories of the target with five eye traces. *Below* are corresponding component plots of: horizontal position, horizontal velocity, vertical position, and vertical velocity. Note the smoothness and consistency of pursuit

sinusoid was added to either the same or the orthogonal axis, with larger effects when the second sinusoid was added to the same axis. In contrast, the addition of a lower-frequency sinusoid had no statistically significant effect on the phase of a higher-frequency component. These ideas are summarized by the following inequalities

$$\text{Phase(Low+Same)} > \text{Phase(Low+Orthogonal)} > 0 > \text{Phase(Low alone)}$$

$$0 > \text{Phase(High alone)} \approx \text{Phase(High+Same)} \approx \text{Phase(High+Orthogonal)}$$

Sum-of-three-sines pursuit

Related, although not identical, results were observed for more complex sum-of-three-sines trajectories. The lead-lag relationship for low- versus high-frequency components was retained, but the gain effects were smaller and less consistent than those observed above. A primary finding was that pursuit was still quite good for these more complex trajectories. Figure 6 shows eye trajectories for the H4H6V7 waveform at 0.05 Hz and 0.15 Hz. Pursuit was smooth and consistent across repetitions of the same trajectory, and, although the initiation points of saccades were more scattered, they were still more common at high-velocity points. Gain (Fig. 7) and phase (Fig. 8) measurements indicated that the monkeys tracked these sum-of-three-sines trajectories with good precision. Means of the gains for individual trajectories (Table 2) for low-, medium-, and high-frequency components were: 0.86, 0.88, and 0.93; while corresponding phase values were: +6°, –2°, and –4° at the three fre-

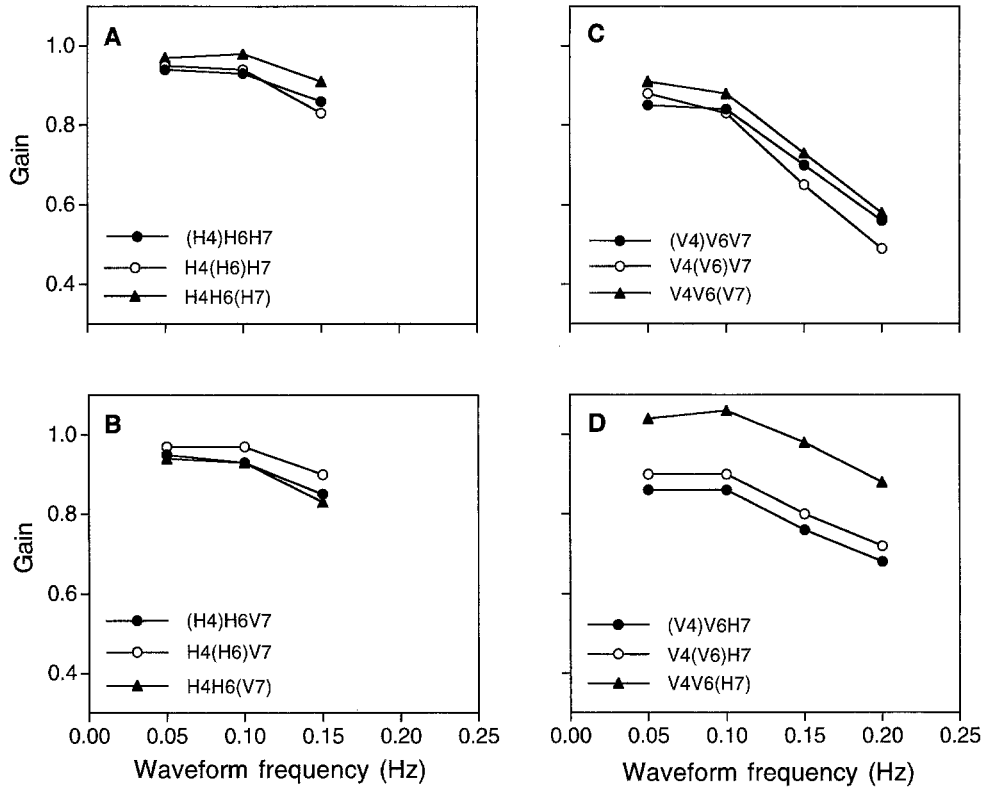

Fig. 7A–D Gain comparisons among high-, medium- and low-frequency components used to create sum-of-three-sines trajectories. *Lines* indicate the gain of low- (*filled circles*), medium- (*empty circles*), and high-frequency (*filled triangles*) components. Data from the same waveform are aligned vertically. Thus, the points at 0.10 Hz correspond to mean gains for three components at 0.40, 0.60, and 0.70 Hz used to construct sum-of-three-sines trajectories at 0.10 Hz. The waveforms analyzed were: **A** H4H6H7, **B** H4H6V7, **C** V4V6V7, **D** V4V6H7

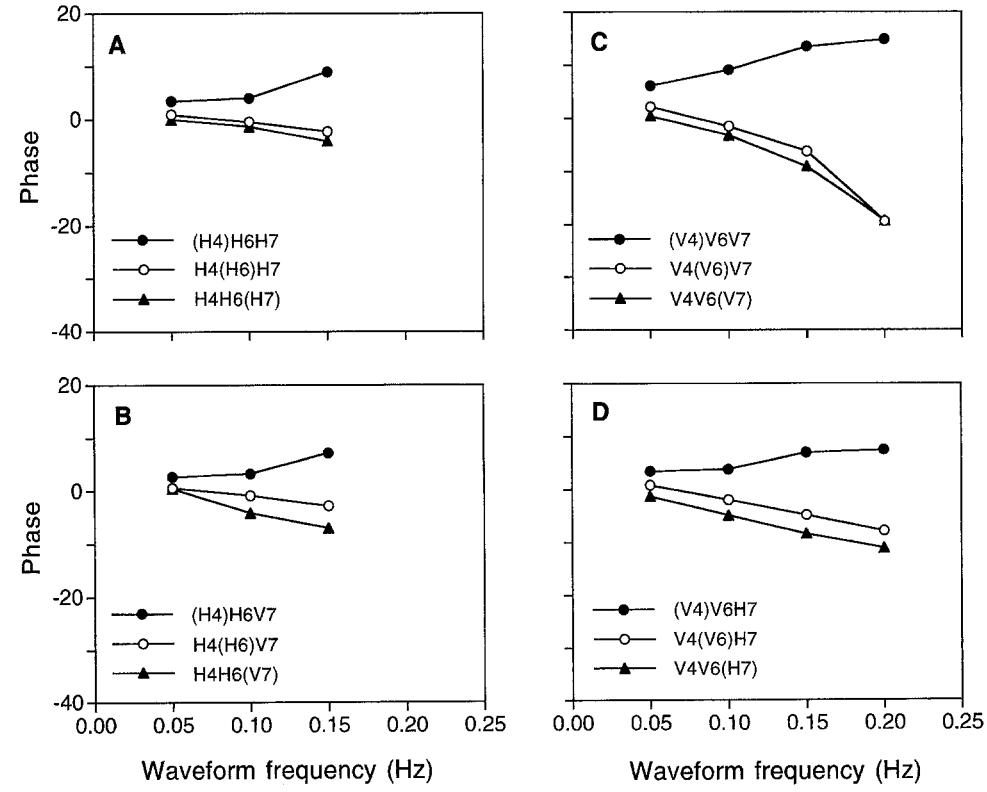

Fig. 8A–D Phase comparisons among high-, medium- and low-frequency components used to create sum-of-three-sines trajectories. Note the consistent phase lead for low-frequency components. Symbols are as in Fig. 7. *Lines* indicate the phase of low- (*filled circles*), medium- (*empty circles*), and high-frequency (*filled triangles*) components. Data from the same waveform are aligned vertically. Thus, the points at 0.10 Hz correspond to mean phases for three components at 0.40, 0.60, and 0.70 Hz used to construct sum-of-three-sines trajectories at 0.10 Hz. Components used to compute phases are in *parentheses*. The waveforms analyzed were: **A** H4H6H7, **B** H4H6V7, **C** V4V6V7, **D** V4V6H7

quencies used for quantitative analysis: 0.05, 0.10, and 0.15 Hz. These gain and phase values are somewhat higher than those observed for sum-of-two-sines pursuit, in part, because the components used to construct these trajectories were somewhat lower in frequency. These frequencies were used because the monkeys would not perform at higher frequencies (see Materials and methods).

The most striking differences among components were observed for phase (Fig. 8). The lag-lead relation-

Table 2 Two-way ANOVA results for the sum-of-three-sines experiments. Values on the left side of the table are means (based on three frequencies×two monkeys×five repetitions) for performance along specific trajectories across a standard set of waveform frequencies at 0.05, 0.10, and 0.15. Each mean corresponds to a specific curve for component gain (Fig. 7), component phase (Fig. 8), interaction gain (Fig. 9), and interaction phase (Fig. 10). Each line of the table corresponds to one of the 16 ANOVA tests that were performed. See Table 1 for more detail

	Trajectory	Components					Trajectory		Frequency	
		Low	Medium	High	HSD	Ms error	$F_{2,81}$	P	$F_{2,81}$	P
Gains	H4H6H7	0.913	0.907	0.958	0.035	0.003	7.2	0.00	27.4	0.00
	H4H6V7	0.917	0.953	0.899	0.027	0.002	12.7	0.00	39.6	0.00
	V4V6V7	0.795	0.785	0.839	NS	0.014	1.7	0.18	21.8	0.00
	V4V6H7	0.825	0.862	1.024	0.052	0.007	48.4	0.00	13.8	0.00
Phases	H4H6H7	5.2	−0.8	−2.0	1.6	6.9	64.6	0.00	1.0	0.39
	H4H6V7	3.8	−1.2	−3.6	1.8	8.8	48.0	0.00	7.5	0.00
	V4V6V7	9.5	−2.1	−4.0	2.5	16.7	95.7	0.00	5.1	0.01
	V4V6H7	4.8	−2.0	−4.7	1.5	6.2	114.9	0.00	11.7	0.00
	Trajectory	Interactions								
		Alone	+Same	+Orthogonal						
Gains	(H4)H6	0.937	0.913	0.913	NS	0.002	2.6	0.08	28.5	0.00
	H4(H6)	0.984	0.907	0.951	0.028	0.002	21.5	0.00	27.5	0.00
	(V4)V6	0.808	0.795	0.819	NS	0.012	0.4	0.69	12.2	0.00
	V4(V6)	0.864	0.785	0.859	0.063	0.010	5.8	0.00	18.1	0.00
Phases	(H4)H6	2.5	5.2	3.8	0.9	2.1	26.0	0.00	48.5	0.00
	H4(H6)	−1.4	−0.8	−1.2	NS	7.9	0.4	0.66	15.6	0.00
	(V4)V6	6.2	9.5	4.8	1.6	6.7	25.6	0.00	22.5	0.00
	V4(V6)	−2.8	−2.1	−2.0	NS	13.6	0.4	0.67	29.4	0.00

ship associated with high- versus low-frequency components was very clear for every waveform and at every frequency. High- and medium-frequency components had phase lags, while low-frequency components exhibited clear and consistent phase leads. Gain differences between components were weaker than differences between sum-of-two-sines components (Fig. 7), but the high-frequency component was still tracked with the highest gain for all but the H4H6V7 trajectory where the high-frequency component was along the vertical axis. The largest gain differences were observed for the V4V6H7 trajectory with a horizontal high-frequency component.

One goal of this investigation of sum-of-three-sine combinations was to study the effects of adding a single sinusoid to a trajectory that was already complex. This was done by computing gain and phase values for the waveforms H4H6 and V4V6 presented alone and in combination with the higher-frequency components H7 and V7 on the same or orthogonal axis. The results in terms of component gain are illustrated in Fig. 9. The top panels of Fig. 9 show curves that are statistically identical (Table 2). This indicates that the addition of high-frequency components, H7 or V7, did not affect the gain of the lower-frequency components (H4)H6 and (V4)V6. This result does not contradict previous results based upon sum-of-two-sine combinations, because (H4)H6 and (V4)V6 have already been suppressed by their combination with H6 and V6. The bottom panels illustrate findings for the intermediate-frequency components H4(H6) and V4(V6). Both showed statistically significant reductions in gain when an additional sinusoid was added along the same axis. When an additional sinusoid was added to the orthogonal axis, smaller decreases were observed that were statistically significant for H4(H6), but were not significant for V4(V6).

In contrast to gain interactions that only occurred for the intermediate-frequency components, phase interactions were still strongest for low-frequency components. The top panels of Fig. 10 show significant differences (Table 2) between the phases of the (H4)H6 and (V4)V6 components presented alone compared with their combination with H7 and V7 components on the same or orthogonal axis. In both cases the largest changes were observed for the same-axis additions, (H4)H6H7 and (V4)V6V7. Orthogonal-axis additions resulted in an increase in phase lead for (H4)H6V7 and a slight decrease in phase lead for (V4)V6H7. In each panel, all three curves indicate leads, because these low-frequency components are always combined with higher-frequency components. The effects on H4(H6) and V4(V6) of same- and orthogonal-axis additions shown in the bottom panels were not statistically significant.

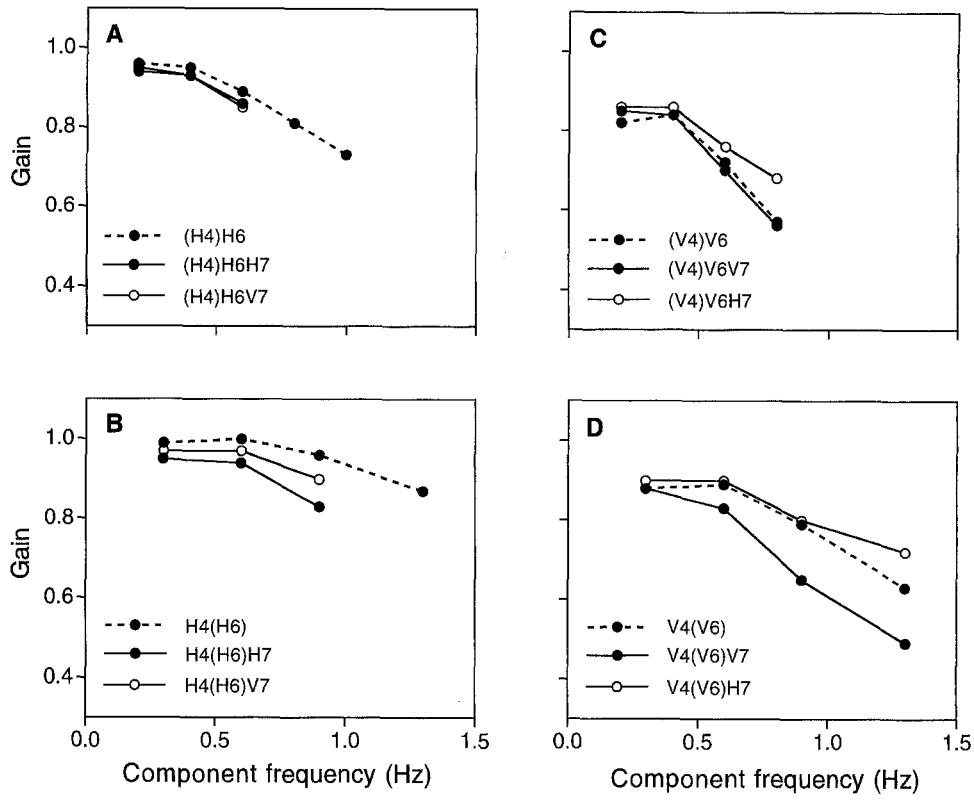

Fig. 9A–D Gain effects on complex sum-of-two-sines pursuit when a third sinusoid is added to either the orthogonal or the same axis. *Three lines* in each panel show the gain of either a high- or low-frequency component for sum-of-two-sines trajectories (*dashed line with filled circles*) and how their gain is affected by the addition of a third sinusoid on the same axis (*solid line with filled circles*), or the orthogonal axis (*solid line with empty circles*). Components used to compute gains are in *parentheses*. The base sum-of-two-sines waveforms for each panel are: **A** (H4)H6, **B** H4(H6), **C** (V4)V6, **D** V4(V6)

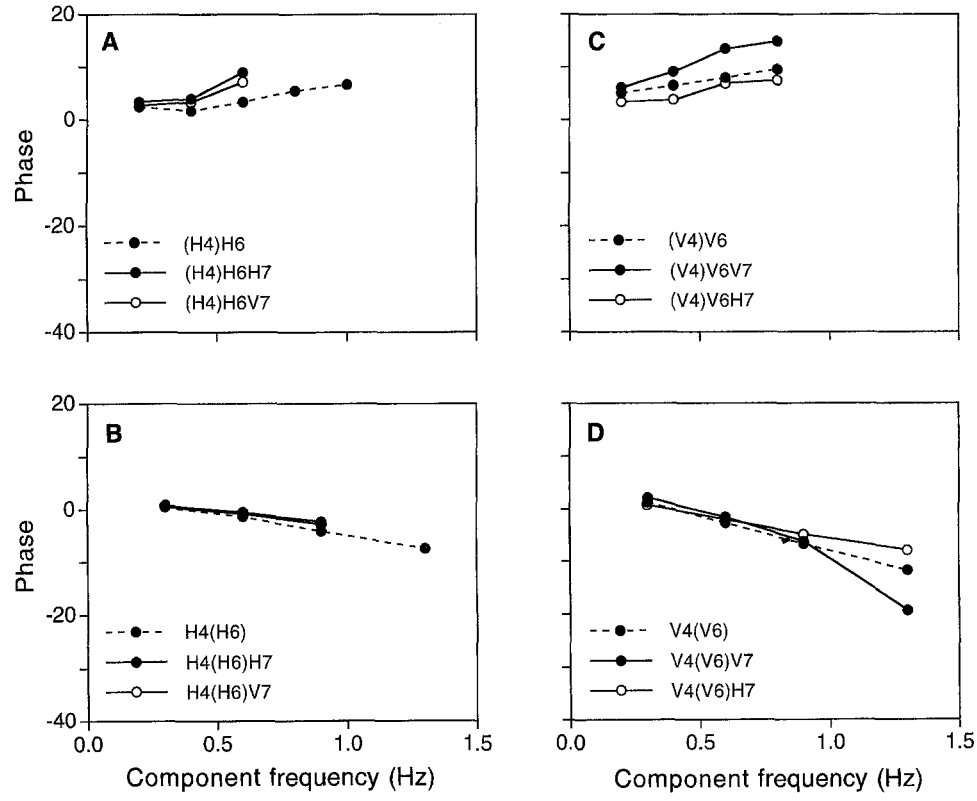

Fig. 10A–D Phase effects on complex sum-of-two-sines pursuit when a third sinusoid is added to either the orthogonal or the same axis. *Three lines* in each panel show the phase of either a high- or low-frequency component for sum-of-two-sines trajectories (*dashed line with filled circles*) and how their phase is affected by the addition of a third sinusoid on the same axis (*solid line with filled circles*) or the orthogonal axis (*solid line with empty circles*). Components used to compute phases are in *parentheses*. The base sum-of-two-sines waveforms for each panel are: **A** (H4)H6, **B** H4(H6), **C** (V4)V6, **D** V4(V6)

Discussion

Predictive pursuit

Both monkeys were able to track both sum-of-two-sines and sum-of-three-sines trajectories with remarkable accuracy at intermediate frequencies before pursuit broke down. Mean values for component gain averaged 0.83, while the mean phase magnitude was 6°. This accuracy is not possible using simple feedback control systems that make trajectory changes after delays that have been estimated at 100–200 ms (Rashbass 1961; Robinson

1965; Fuchs 1967; Becker and Fuchs 1984; Leung et al. 1994; Leung and Kettner 1995). While simple feedback control works well for systems with feedback delays that are small relative to changes in input, the feedback delays associated with visual pursuit are too long to explain the high quality of pursuit that was observed in these and other experiments. This point has been made before with regard to low-frequency components of complex pursuit in terms of phase leads (Dallos and Jones 1963; Yasui and Young 1984) and with regard to the highest-frequency components in terms of gain and phase (Barnes et al. 1987; Barnes and Ruddock 1989). We have now observed both effects in monkeys with an ultimate aim of studying the neural mechanisms of predictive pursuit along complex trajectories. We have also extended previous analyses of horizontal pursuit to vertical and two-dimensional pursuit.

Differential processing of high- and low-frequency components

The trajectories that were tracked in the present study were created by applying two or three sinusoids in various combinations to horizontal and vertical axes. The resulting trajectories were relatively complex but still had the advantage of allowing a breakdown of pursuit performance into sinusoidal components for quantitative analysis. There were clear and consistent differences in the processing of these components that suggested two types of tracking control. High-frequency components tended to be tracked with a higher gain and a phase lag, while low-frequency components were processed with a lower gain and a phase lead.

Comparisons between single sinusoids and components of the same frequency and amplitude suggested the following generalization about what occurs when sinusoids are combined: tracking of the high-frequency component is relatively less affected by the combination; it retains its high gain and phase lag with relatively little modification. In contrast, the low-frequency component is more strongly altered: its gain is reduced, and its phase relationship with the target switches from lag to lead. Thus, the clear differences in high- versus low-frequency component tracking result primarily from changes in the tracking of the low-frequency component.

High- versus low-frequency gain and phase differences have been noted by other investigators for sum-of-sines stimuli restricted to the horizontal axis in humans (Barnes et al. 1987; Barnes and Ruddock 1989). They have argued that the tracking of a sum-of-sines trajectory is dominated by the highest-frequency component, while tracking performance for other components are reduced in gain. With some provisos, we have extended these results to vertical trajectories and to two-dimensional trajectories. In light of the present experiments, we would add the idea that the highest-frequency component appears to be tracked like a single sinusoid, and that the low-frequency component is tracked in a different but not necessarily reduced mode. After all, a phase lead may indicate predictive tracking that is beneficial to overall tracking performance (Yasui and Young 1984). In addition, while we see changes in gain for the low-frequency component, the most consistent changes are in phase.

Horizontal versus vertical pursuit

Significantly better tracking was observed for trajectories restricted to the horizontal compared with the vertical axis, a result that has also been reported for human pursuit (Collewijn and Tamminga 1984; Baloh et al. 1988). This suggests a clear asymmetry in the systems that control pursuit. A neural substrate for this difference is provided by physiological studies that support the idea of independent horizontal and vertical channels for eye movement control. Recording and stimulation studies indicate that distinct brainstem regions are related to horizontal and vertical eye control (Fuchs and Kimm 1975; Chubb and Fuchs 1982; Chubb et al. 1984; Tomlinson and Robinson 1984; Langer et al. 1986; McCrea et al. 1987a,b; Mustari and Fuchs 1989; McFarland and Fuchs 1992; Scudder and Fuchs 1992). There is also evidence that the flocculus of the cerebellum, which has been implicated in the control of smooth pursuit (Zee et al. 1981), is divided into separate horizontal and vertical zones based on electrical stimulation, anatomical and neural recording studies (Miles et al. 1980; Balaban et al. 1981; Balaban and Watanabe 1984; Lisberger and Fuchs 1978a, b; Belknap and Noda 1987; Stone and Lisberger 1990a, b; Sato and Kawasaki 1991). Many of these results may reflect the control of specific ocular muscles associated with horizontal and vertical eye movement.

One initial reason for conducting this study was to examine interactions between horizontal and vertical pursuit. Because of the anatomical and functional evidence for a division between horizontal and vertical eye movement systems, it was logically possible that horizontal and vertical eye movement behaviors would also be independent. This hypothesis was not supported by the present experiments. There were clear effects of presentation axis that would not have occurred if horizontal and vertical pursuit were independent. This finding is consistent with other physiological data from brain regions that send visual information to the cerebellum and other brain structures controlling eye movements. For example, cerebellar areas controlling eye movements receive mossy fiber inputs from the dorsolateral pontine nuclei which, in turn, receive input from the middle temporal and medial superior temporal areas of the neocortex. Neurons in these three regions show preferred directional tuning for a wide range of visual movements (Maunsel and Van Essen 1983; Mustari et al. 1988; Kawano et al. 1992, 1994). In addition, Purkinje cell responses to vestibular stimulation suggest deviations from pure horizontal or pure vertical tuning (Fukushima et al. 1990; Powell et al. 1992, 1994; Graf et al. 1993) and receive a wide range of afferent fiber inputs (Sato et al. 1983).

These interactions are not due to saturation nonlinearities in any simple sense because they were observed

across a wide range of trajectory velocities, as they were observed for both high- and low-frequency components and they acted both to increase and decrease gain and phase values. By definition, none of these nonlinear interactions can be generated by linear models. Some models (Robinson et al. 1986; Krauzlis and Lisberger 1989) have introduced saturation nonlinearities, but do not address interactions between axes. Although it is generally possible to approximate the behavior of a nonlinear system by a linear model for some local subset of inputs and outputs, the range of normal pursuit behaviors described in this report appears to exceed these boundaries. In particular, predictive processes that vary with component frequency are not easily modeled by linear systems.

Even so, we did observe a limited independence between horizontal and vertical control. We found that same-axis interactions between waveforms were stronger than orthogonal-axis interactions. Put another way, two-dimensional trajectories were tracked with more accuracy than one-dimensional trajectories created with the same components, albeit on different axes. If one discards the notion that distinct brain systems control horizontal versus vertical pursuit, these results may also be explainable in terms of two-dimensional trajectory variables. For example, the two-dimensional trajectories appeared smoother to us than the one-dimensional trajectories. In a preliminary study (Kettner et al. 1994) we have quantified this observation by computing the mean variance of the waveform velocity for both one- and two-dimensional trajectories created from same-frequency components. The results show that velocity is more variable for the one-dimensional trajectories. This could explain why these trajectories are more difficult to track and why same-axis interactions are stronger than orthogonal-axis interactions.

Acknowledgements We thank Mary Giswold for technical assistance. This study was supported by grants MH 48185 and T32 DC00015-13.

References

Bahill AT, McDonald JD (1983) Smooth pursuit eye movements in response to predictable target motions. Vision Res 23:1573–1583

Balaban CD, Watanabe E (1984) Functional representation of eye movements in the flocculus of monkeys (*Macaca fuscata*). Neurosci Lett 49:199–205

Balaban CD, Ito M, Watanabe E (1981) Demonstration of zonal projections from the cerebellar flocculus to vestibular nuclei in monkeys (*Macaca fuscata*). Neurosci Lett 27:101–105

Baloh RW, Yee RD, Honrubia V, Jacobson K (1988) A comparison of the dynamics of horizontal and vertical smooth pursuit in normal human subjects Aviat Space Environ Med 59:121–124

Barnes GR, Ruddock CJS (1989) Factors affecting the predictability of pseudo-random motion stimuli in the pursuit reflex of man. J Physiol (Lond) 408:137–165

Barnes GR, Donnelly SF, Eason RD (1987) Predictive velocity estimation in the pursuit reflex response to pseudo-random and step displacement stimuli in man. J Physiol (Lond) 389:111–136

Becker W, Fuchs AF (1984) Prediction in the oculomotor system: smooth pursuit during transient disappearance of a visual target. Exp Brain Res 57:562–575

Belknap DB, Noda H (1987) Eye movements evoked by microstimulation in the flocculus of the alert macaque. Exp Brain Res 67:352–362

Chubb MC, Fuchs AF (1982) Contribution of y group of vestibular nuclei and dentate nucleus of cerebellum to generation of vertical smooth eye movements. J Neurophysiol 48:75–99

Chubb MC, Fuchs AF, Scudder CA (1984) Neuron activity in monkey vestibular nuclei during vertical vestibular stimulation and eye movements. J Neurophysiol 52:724–742

Collewijn H, Tamminga EP (1984) Human smooth and saccadic eye movements during voluntary pursuit of different target motions on different backgrounds. J Physiol (Lond) 351:217–250

Collewijn H, Van der Mark F, Jansen TC (1975) Precise recording of human eye movements. Vision Res 15:447–450.

Dallos PJ, Jones RW (1963) Learning behavior of the eye fixation control system. IEEE Trans Automat Control 8:218–227

Fuchs AF (1967) Saccadic and smooth pursuit eye movements in the monkey. J Physiol (Lond) 191:609–631

Fuchs AF, Kimm J (1975) Unit activity in vestibular nucleus of the alert monkey during horizontal angular acceleration and eye movement. J Neurophysiol 38:1140–1161

Fukashima K, Perlmutter SI, Baker JF, Peterson BW (1990) Spatial properties of second-order vestibulo-ocular relay neurons in the alert cat. Exp Brain Res 81:462–478

Graf W, Baker J, Peterson BW (1993) Sensorimotor transformation in the cat's vestibuloocular reflex system. I. Neuronal signals coding spatial coordination of compensatory eye movements. J Neurophysiol 70:2425–2441

Judge SJ, Richmond BJ, Chu FC (1980) Implantation of magnetic search coils for measurement of eye position: an improved method. Vision Res 20:535–538

Kawano K, Shidara M, Yamane S (1992) Neuronal activity in dorsolateral pontine nucleus of alert monkey during ocular following responses. J Neurophysiol 67:680–703

Kawano K, Shidara M, Watanabe Y, Yamane S (1994) Neuronal activity in cortical area MST of alert monkey during ocular-following responses. J Neurophysiol 71:2305–2324

Kettner RE, Leung H-C, Giswold ME, Peterson BW (1994) Two dimensional smooth pursuit eye movements during tracking of double sine waves in monkey. Soc Neurosci Abstr 20:1193

Kowler E, Steinman RM (1979) The effect of expectations on slow oculomotor control. I. Periodic target steps. Vision Res 19:619–632

Krauzlis RJ, Lisberger SG (1989) A control systems model of smooth pursuit eye movements with realistic emergent properties. Neural Comp 1:116–122

Langer T, Kaneko CRS, Scudder CA, Fuchs AF (1986) Afferents to the abducens nucleus in the monkey and cat. J Comp Neurol 245:379–400

Leung H-C, Kettner RE (1995) Predictive control of smooth pursuit eye movements along complex two-dimensional trajectories in monkey. Soc Neurosci Abstr 21:140

Leung H-C, Kettner RE, Giswold ME, Peterson BW (1994) Two dimensional smooth pursuit eye movements during circular tracking and perturbations in monkey. Soc Neurosci Abstr 20:1193

Lisberger SG, Fuchs AF (1978a) Role of primate flocculus during rapid behavioral modification of vestibuloocular reflex. I. Purkinje cell activity during visually guided horizontal smooth-pursuit eye movements and passive head rotation. J Neurophysiol 41:733–763

Lisberger SG, Fuchs AF (1978b) Role of primate flocculus during rapid behavioral modification of vestibuloocular reflex. II. Mossy fiber firing patterns during horizontal head rotation and eye movement. J Neurophysiol 41:764–777

Lisberger SG, Evinger C, Johanson GW, Fuchs AF (1981) Relationship between acceleration and retinal image velocity during foveal smooth pursuit in man and monkey. J Neurophysiol 46:229–249

Maunsel JHR, Van Essen DC (1983) Functional properties of neurons in middle temporal visual area of the macaque monkey. I. Selectivity for stimulus direction, speed, and orientation. J Neurophysiol 49:1127–1147

McCrea RA, Strassman A, May E, Highstein SM (1987a) Anatomical and physiological characteristics of vestibular neurons mediating the horizontal vestibulo-ocular reflex in the squirrel monkey. J Comp Neurol 264:547–570

McCrea RA, Strassman A, Highstein SM (1987b) Anatomical and physiological characteristics of vestibular neurons mediating the vertical vestibulo-ocular reflex in the squirrel monkey. J Comp Neurol 264:571–594

McFarland JL, Fuchs AF (1992) Discharge patterns in nucleus prepositus hypoglossi and adjacent medial vestibular nucleus during horizontal eye movement in behaving macaques. J Neurophysiol 68:319–332.

Miles FA, Fuller JH, Braitman DJ, Dow BM (1980) Long-term adaptive changes in primate vestibuloocular reflex. III. Electrophysiological observations in flocculus of normal monkeys. J Neurophysiol 43:1437–1476

Mustari MJ, Fuchs AF (1989) Response properties of single units in the lateral terminal nucleus of the accessory optic system in the behaving primate. J Neurophysiol 61:1207–1220

Mustari MJ, Fuchs AF, Wallman J (1988) Response properties of dorsolateral pontine units during smooth pursuit in the rhesus macaque. J Neurophysiol 60:664–686.

Pola J, Wyatt H (1980) Target position and velocity: the stimuli for smooth pursuit eye movements. Vision Res 20:523–534

Powell KD, Quinn KJ, Barke LD, Peterson BW (1992) Spatial properties of flocculus neurons in the decerebrate cat. Soc Neurosci Abstr 18:406

Powell KD, Killian JE, Peterson BW (1994) Maximum activation direction and visual-vestibular interaction of flocculus purkinje cells in alert cats. Soc Neurosci Abstr 20:1746

Press WH, Teukolsky SA, Vetterling WT, Flannery BP (1992) Numerical recipes in C: The art of scientific computing, 2nd edn. Cambridge University Press, Cambridge

Rashbass C (1961) The relationship between saccadic and smooth tracking eye movements. J Physiol (Lond) 159:326–338

Robinson DA (1963) A method of measuring eye movement using a scleral search coil in a magnetic field. IEEE Trans Biomed Electron 10:137–145

Robinson DA (1965) The mechanics of human smooth pursuit eye movements. J Physiol (Lond) 180:569–591

Robinson DA, Gordon JL, Gordon SE (1986) A model of the smooth pursuit eye movement system. Biol Cybern 55:43–57

Sato Y, Kawasaki T (1991) Identification of the purkinje cell/climbing fiber zone and its target neurons responsible for eye-movement control by the cerebellar flocculus. Brain Res Brain Res Rev 16:39–64

Sato Y, Kawasaki T, Ikarashi (1983) Afferent projections from the brainstem to the three floccular zones in cats. II. mossy fiber projections. Brain Res 272:37–48

Scudder CA, Fuchs AF (1992) Physiological and behavioral identification of vestibular nucleus neurons mediating the horizontal vestibuloocular reflex in trained rhesus monkeys. J. Neurophysiol 68:244–264.

Stone LS, Lisberger SG (1990a) Visual responses of purkinje cells in the cerebellar flocculus during smooth pursuit eye movements in monkeys I. Simple spikes. J Neurophysiol 63(5):1241–1261

Stone LS, Lisberger SG (1990b) Visual responses of purkinje cells in the cerebellar flocculus during smooth pursuit eye movements in monkeys II. Complex spikes. J Neurophysiol 63:1262–1275

Tomlinson RD, Robinson DA (1984) Signals in vestibular nucleus mediating vertical eye movements in the monkey. J Neurophysiol 51:1121–1136.

Van den Berg AV (1988) Human smooth pursuit during transient perturbations of predictable and unpredictable target movement. Exp Brain Res 72:95–108

Winer BJ, Brown DR, Michels KM (1991) Statistical principles in experimental design, 3rd edn. McGraw-Hill, New York

Yasui S, Young LR (1984) On the predictive control of foveal eye tracking and slow phases of optokinetic and vestibular nystagmus. J Physiol (Lond) 347:17–33

Zee DS, Atsumi Y, Butler PH, Güçer G (1981) Effects of ablation of flocculus and paraflocculus on eye movements in primate. J Neurophysiol 46:878–899